JOURNAL OF APPLIED ELECTROCHEMISTRY 2 (1972) 105–112

On the distribution of current generation in porous gas electrodes

K. J. EULER

Fachbereich Physik der Gesamthochschule Kassel, Germany

Received 4 September 1970 and in revised form 20 May 1971

In the active layer of porous gas electrodes, the spatial distribution of energy generation is determined by several interacting factors, e.g. pore statistics, distribution of active sites, and a set of correlated transport equations. After a short introduction to the problem, it is shown that the transport phenomena can, in this case, be treated in a very simplified manner. In particular, the specific electron resistance can be neglected. Restriction of gas supply can be described by a formalistic gas resistance ρ_g. Thus, the interaction of the different transport parameters can be treated by considering purely electrical models. The relative magnitudes of the different parameters, in the case under study, are of such an order that finally it is only necessary to consider two of them: the specific ionic resistivity of the porous electrode filled partly with liquid electrolyte, and a special parameter p which describes the overvoltage in the region between gaseous phase and electrolyte. As a result, the spatial distribution of current generation can be indicated in the form of analytical expressions and diagrams. One also obtains values of the penetration depth of current generation which do not disagree with practical experience.

1. Introduction

At bulk electrodes having smooth surfaces, the electrochemical generation of electric energy from reacting gases proceeds very slowly. It is characterized by a current density i of only a few microamperes per square centimetre. Therefore, porous partly wetted electrodes are used, having large inner surfaces and numerous microscopic triphase zones generating electricity. If the electrode matrix has the specific inner surface $\omega(\mathrm{cm^2 cm^{-3}})$, the very small primary current density i at the outer surface of the electrode having the finite thickness S should be related to the considerably higher geometrical current density i_s, by:

$$i_s = i\omega S \qquad (1)$$

However, increasing the thickness beyond a critical value S_1, of the order of a few millimetres, will no longer increase i_s. Taking into account volume, weight and cost, the electrode will become, at a certain thickness S_2, the most economic one. In general S_2 is smaller than S_1.

The problem we tried to solve in this paper was to find a method for the evaluation of the spatial distribution of current generation inside porous gas electrodes. Furthermore, we tried to define a 'penetration depth' of the current generation, as the useful thickness of the working electrode layer. And of course we had to find out the parameters governing the behaviour of this type of electrode.

2. General theory

Porous gas electrodes consist of a solid porous matrix manufactured in most cases by pressing or sintering procedures. The materials in use are metal or carbon powders, with or without binding agents, and with or without current collectors incorporated. The pores of the matrix are partly wetted with a liquid electrolyte, partly filled with a reacting gas. To effect this, hydrophobic agents may be applied or a sandwich-type electrode with stepped pore diameter used [1].

Incorporated into the solid porous matrix are grains of catalyst [2], or the inner surface is coated with an electrochemically active layer. Inert gas impurities are not considered here.

Thus, the porous gas electrode comprises at least three different phases which form a thoroughly mixed web of electron-, ion- and gas-carrying threads. In most cases, one or more of these phases are composite.

2.1. *Transport phenomena*

Within this triple web, the electrochemical reaction takes place. As an example, the anodic oxidation of hydrogen in an alkaline solution can simply be written:

$$H_2 + 2\,OH^- \rightarrow 2\,H_2O + 2\,e^- - Q$$

Hydrogen and OH^- ions are consumed, water, electrons and heat Q are formed. The reaction therefore implies several transport phenomena:

(1) gas supply, due to pressure difference and diffusion
(2) migration of OH^- ions
(3) motion of electrolyte, due to water formation
(4) penetration of water vapour into the gas-filled pores
(5) motion of the triphase zones, due to concentration changes
(6) electron conduction
(7) heat removal, by conduction, evaporation and convective transfer.

Even excluding transients, we have to expect complicated and interrelated effects, e.g. spatial distribution of gas pressure, electrolyte concentration, etc., see Table 1.

These fluxes, of course, can be described by appropriate equations: the Poisson equation, the Stokes–Navier equation, Fick's diffusion law, and the equation of heat conduction. However, the specific parameters depend on electrolyte concentration, temperature and pressure. The heat conduction will be influenced by evaporation and convective cooling. Non-constant coefficients link the variables in the differential equations, and so give a complicated set of conditions to be fulfilled simultaneously. An analytical treatment only becomes possible,

Table 1. Factors influencing current distribution in porous gas electrodes. Dotted: less important

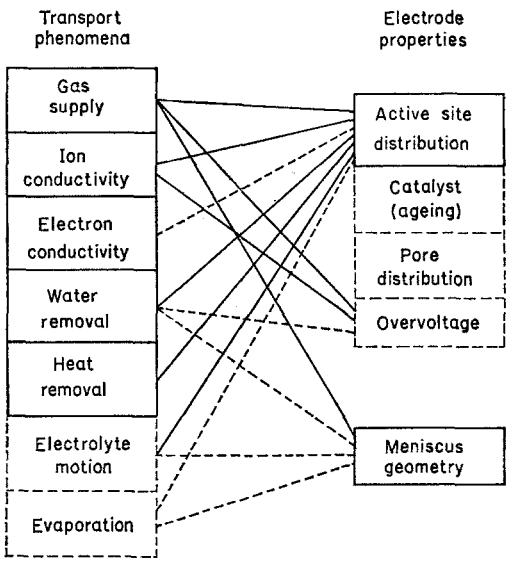

if at all, after the introduction of extensive simplifications.

2.2. *Statistics of triphase zones*

Another, no less important, factor is the statistics of the 'active sites' inside the porous matrix. To generate a differential electric current di, we need sufficient catalytic activity and the formation of a microscopic triphase zone. Meniscus position, electrolyte film thickness and the formation, as well as the motion, of insulating gas bubbles depend on viscosity and gas pressure drop inside the pores. Thus, the distribution of triphase zones, though mainly caused by the geometrical arrangement of the electrode elements, will be influenced by the transport phenomena. An even approximate analytical evaluation of the triphase zone distribution seems at present impossible. However, it can be measured. Ageing and poisoning of catalysed gas electrodes can considerably change the statistics of active sites during electrode life.

2.3. *Current distribution in the single pore*

Since the total current i_s is formed in differential parts di by a great number of microscopic triphase zones, we have to investigate how far the

current distribution in the single microscope triphase zone influences the macroscopic current distribution in the electrode. It is evident that the amount of current set free in each triphase zone will influence the total electrode current. However, this is not within the scope of this paper. It depends only on correct choice and handling of catalyst and matrix material but not on electrode thickness.

The current conversion in the immediate vicinity of individual triphase zones has been studied recently by several authors [2–9], whereas the aforementioned macroscopic distribution in hydrophilic sandwich type electrodes has not been considered before. Although the distribution of current in a single pore, or in a single triphase zone, may be influenced by transport phenomena, *a priori*, we cannot exclude the possibility that interactions exist between the statistical arrangement of the microscopic triphase zones and the current distribution in a single triphase zone. However, this has not yet been proven.

3. Simplifications and restrictions

In this section we try to introduce possible simplifications.

3.1 *Electrode geometry*

We restrict ourselves to flat electrodes having finite thickness S, small compared with lateral dimensions (see Fig. 1). The pores in the cover layer are supposed to be completely filled with electrolyte and we suppose, furthermore, that hydrostatic pressure differences can be neglected.

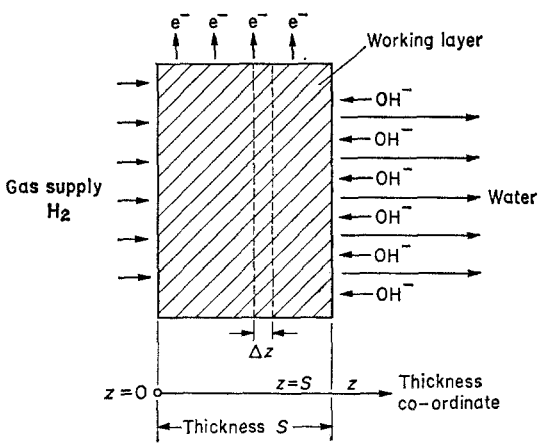

Fig. 1. Geometrical arrangement of the semi-infinite porous double layer electrode. The cover layer acts only as a resistor in the electrolyte path.

3.2. *Electron resistivity*

The specific ion resistivity is in the order of 10 to 100 Ω cm whereas macroscopic electron resistivity in most cases is lower than 0·001 Ω cm. Taking into account electrode thickness (ion path) of 0·1 to 1 cm and lateral electrode dimensions (electron path) of 10 to 30 cm, we may ignore electron resistance.

3.3. *Temperature and pressure fields*

Flat porous metal electrodes in free electrolyte exhibit high heat dissipation because heat transport proceeds perpendicular to a relatively thin plate. Behind the electrode the heat is removed by the aqueous (and in most cases streaming) electrolyte. Therefore, metal electrodes can be regarded as isothermal. In carbon electrodes, a certain temperature gradient will occur. However, a non-constant temperature introduces serious complications. Therefore we accept the small uncertainty in the results which will arise from ignoring it.

Pressure gradients in the gas-filled pores can be neglected if inert impurities are absent, or if the electrode has been purged sufficiently. Diffusion gradients can also be neglected as shown below.

We intend to compare the independently measurable diffusion coefficient with a resulting ion resistivity.

Using the Einstein equation $D = bkT\mathrm{e}$ a 'gas resistivity' ρ_g can be defined:

$$\frac{1}{\rho_g} = n N b e = D n N e^2/kTf \qquad (2)$$

where

N [cm^{-3}] = carrier density
n = number of elementary charges per carrier
b = [cm^2/V s] mobility
e = $1{\cdot}61 \times 10^{-19}$ (A s)
D = [cm^2 s^{-1}] diffusion coefficient
$kT \cdot \mathrm{e}^{-1}$ = 25 mV at room temperature

$f \approx 4$; a geometrical factor including porosity, tortuosity, etc.

The use of this expression is valid because the diffusion constant D of the neutral gas molecules has been replaced in a rather formalistic manner by a fictive mobility b of not really existing charge carriers, but which however represent the properties of the gas supply. This procedure allows us to represent the different transport phenomena with the help of only one single electric model, see Fig. 2. To be precise, the

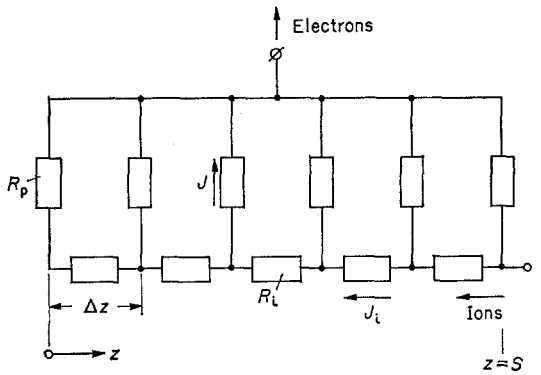

Fig. 2. Resistor chain corresponding to flat porous gas electrodes. Resistors introduced by the gas supply can be neglected.

Einstein equation applies only to conductors having equal mobilities of all carriers. At fuel cell electrodes, K^+ and OH^- ions are usually involved, the mobilities of which differ considerably from each other. However, only an estimate is necessary in the framework of this investigation. The approximation therefore seems sufficient. Inserting the following quantities into Equation (2):

$D > 0{\cdot}1$ (valid for gases at room temperature under nearly atmospheric pressure)
$N \approx 5{\cdot}3 \times 10^{19}$ cm^{-3} room temperature, pressure 2 kp cm^{-2}
$n = 1$
$e = 1{\cdot}61 \times 10^{-19}$ A s
$f \approx 4$

we obtain $0{\cdot}01 < \rho_g < 0{\cdot}1$ Ω cm.

The ionic resistivity $\bar{\rho}_i$ inside the working layer can be easily estimated. Porosity is around 50%, and about 15% of the pores is filled with electrolyte, 6 N KOH at 60°C. Taking into consideration a tortuosity factor of 1·5, the final ionic resistivity can be calculated to be $\rho_i \approx 20$ Ω cm. This result agrees well with experimental results.

Since $\rho_g \ll \bar{\rho}_i$ gas diffusion need not be taken into consideration.

3.4. *Water removal*

Since the water produced in the electrode reaction lowers the ionic conductivity inside the electrode, its effect can be approximately taken into consideration, under steady state conditions, by the introduction of a somewhat elevated ionic resistivity $\bar{\rho}_i$.

4. Resulting transport equation

Introducing the above-mentioned simplifications, there remains only one transport parameter to be considered: the ion resistivity ρ_i. Regarding electrode overvoltage Ψ it may be possible to introduce simply a constant resistance r, related to unit area of the inner surface. Inserting the specific inner surface ω, we define the overvoltage parameter $p = r/\omega$ (Ω cm^3). Then we get $\Psi = r\,i = p\,i_s/S$, having i the current density, i_s the geometrical current density at the surface and S the electrode thickness. Here we must not forget that p and Ψ are not pure electrical magnitudes. The overvoltage contains an ohmic component arising from concentration overvoltage in the adherent electrolyte layer, and furthermore a component caused by the concentration or activity difference of the working gas in the triphase zone with and without current flowing.

As we already know, having carried out a considerable number of investigations on different types of porous electrodes, see (e.g. ref. [11]), p lies in the range $0{\cdot}1 < p < 10$ Ω cm^3. Since Equation (4) is not very sensitive to errors in the values of p, even a rough estimate does not introduce intolerable uncertainties. Also, we know from a thorough study [12], that the linear approximations of the complicated overvoltage functions are quite reasonable.

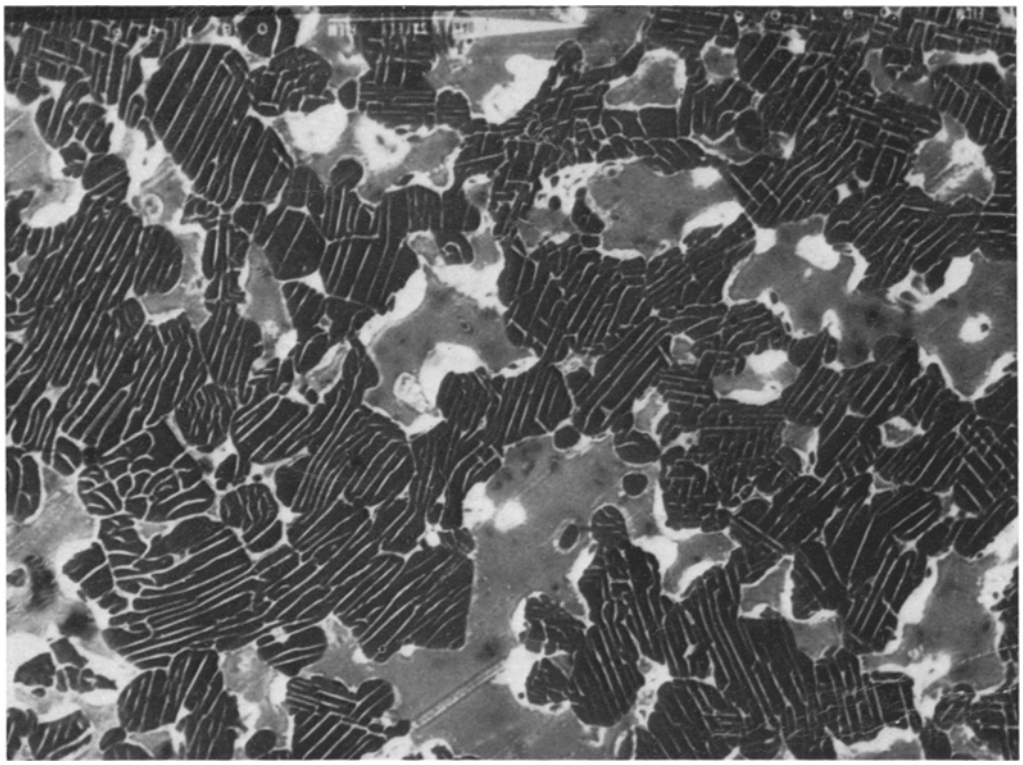

Fig. 3. Texture of sintered nickel electrode before activation. The microgram covers a field of about $70 \times 100\ \mu m$. Dark crystals with white stripes: $NiAl_3$ eutectic, medium grey: pores filled with embedding mass, white: pure nickel, dark spots: impurities.

facing p. 109

The transport behaviour of porous gas electrodes can be described by electrical resistor chains, see for instance [11]. As shown in Fig. 2, ions penetrate the active electrode layer from the right-hand side along a resistor chain. They are successively converted into electrons. The cross resistors R_p simulate the overvoltage. One mesh in Fig. 2 corresponds to a thickness interval Δz; the resistors are:

$$R_i = \rho_i \, \Delta z/A \text{ and } R_p = p/A\Delta z \qquad (3)$$

where A is the surface area of the electrode. Fig. 2 resembles a transmission line having imperfect insulation. If we introduce as abbreviations:

$$C^2 = \rho_i S^2/p \text{ and } C/(S \sinh C) = K \qquad (3a)$$

S = electrode thickness (cm)
ρ_i = ion resistivity (Ω cm)
p = overvoltage parameter (see page 108)

we get finally the expression for the transport component of the current distribution in the flat porous gas electrode:

$$V_t = J(z)/i_s = K \cosh (Cz/S) \qquad (4)$$

$J(z)$ the current generated at the point z per unit of volume, to be measured in A cm^{-3}. The geometrical (surface) current density i_s (A cm^{-2}) has been already defined at the beginning of this paper. The abbreviation K, a constant, is given by the expressions (3a). See also [13].

5. Active site statistics

In general, active sites are mainly preformed by the arrangement of pores and catalyst grains within the electrode. Fig. 3 shows a microgram, covering a field of about 70×100 μm, of sintered and homogenized Raney nickel catalyst before the activation takes place. The dark crystals with narrow white stripes consist of the eutectic $NiAl_3$. During the activation process, the high aluminium content is dissolved. A porous, laminated nickel skeleton remains, which exposes a very large inner surface with a high catalytic activity.

From observations made on a great number of electrodes, we know that there exists a certain statistic distribution of the number of active sites per unit volume, $V_a(z)$, to be measured in cm^{-3}. It depends on grain density variations, grain size distribution, spatial distribution of the activation procedure, flooding of pores, and on poisoning after a prolonged period of work. However, $V_a(z)$ can be regarded as constant. This approximation holds fairly well during the first year of use under rated conditions.

We are not allowed *a priori* to eliminate the influence of z-dependent overvoltage $\Psi(z)$ and ion resistivity $\bar{\rho}_i(z)$. In a preceding paper [14], we investigated the role of these two functions. It has been shown that to a first approximation the site statistics V_a do not depend on transport phenomena.

6. Current distribution in the single triphase zone

In the past, several authors have tried to evaluate the spatial distribution of the current generation in triphase zones, see for instance [2, 3, 6, 7]. The resulting distributions $\Phi(v)$ are related to a co-ordinate v along the single pore, see Fig. 4. The origin of the v-scale is centred on each individual conversion zone. z and v include an angle depending on the geometrical situation of each site.

The distribution $\Phi(v)$ depends markedly on geometrical and physical assumptions, e.g. pore or film geometry, gas diffusion across liquid or across solid phase, surface migration of gas atoms, creeping of electrolyte, electrochemical reaction, its rate-determining step, nature of wastes formed, etc. However, the simple rule that $\Phi(v)$ differs from zero only in a small interval $\pm \Delta v$ on both sides of the coordinate origin, Δv, being comparable to the characteristic 'pore diameter' d, can be regarded as generally valid.

Consequently, each individual conversion site can be regarded as a small differential sphere, the diameter of which is comparable with d. In most cases, d does not exceed 30 μm and remains small as compared with the electrode thickness S.

Inside a single current generating zone, we have to assume, therefore, an unknown current distribution, its shape not being constant with respect to total electrode current and time. In addition the entire current of a single pore depends on the same parameters, see Table 1.

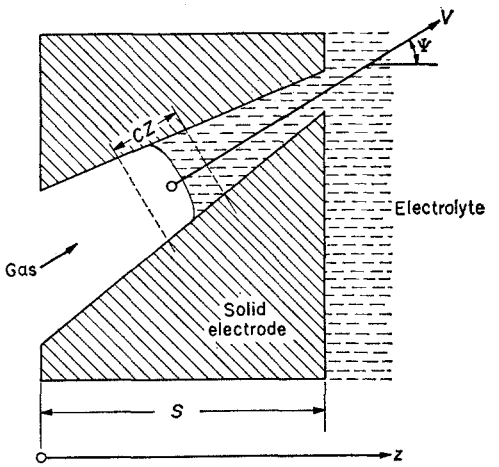

Fig. 4. Relations between electrode co-ordinate z and individual site co-ordinate v.

7. Combination of transport phenomena and electrode properties

We stated above that the resulting transport behaviour $V_t(z)$ and active site distribution V_a exhibit almost no interaction. Therefore we can simply combine $V_t(z)$ and V_a by multiplying together. Taking into account the current I_0 of a single triphase zone and the electrode thickness S we get the resulting current distribution of the active layer of a semi-infinite, flat porous gas electrode

$$V_r(z) = i_r(z)/\bar{\imath} = V_t(z)\, S\, V_a\, \bar{I}_0\, d\tau \qquad (5)$$

The expression indicates the amount of current $i_r(z)$ generated at z, per unit of volume, divided by the mean current, generated per unit volume of the electrode $I = i_s S^{-1}$. The differential $d\tau$ is an element of volume. Since the absolute value of I_0 is not of interest nor can be calculated, we use the reduced current $\bar{I}_0$, which is normalized to fulfil the condition

$$\int_0^S V_r(z)\, dz = 1 \qquad (5a)$$

Thus $V_r(z)$ indicates the fraction of total current $\Delta i_r/i_r$, generated in a certain fraction $\Delta z/S$ (e.g. 0·1 mm) of the entire electrode thickness S. As long as the electrodes are unidimensional and fairly flat, the fractions of current, current densities or current generation per cubic centimetre can be written in an identical manner.

8. Numerical evaluation

Inserting appropriate figures, we get the shape of the resulting current distribution in porous gas electrodes as indicated in Fig. 5. As a result we

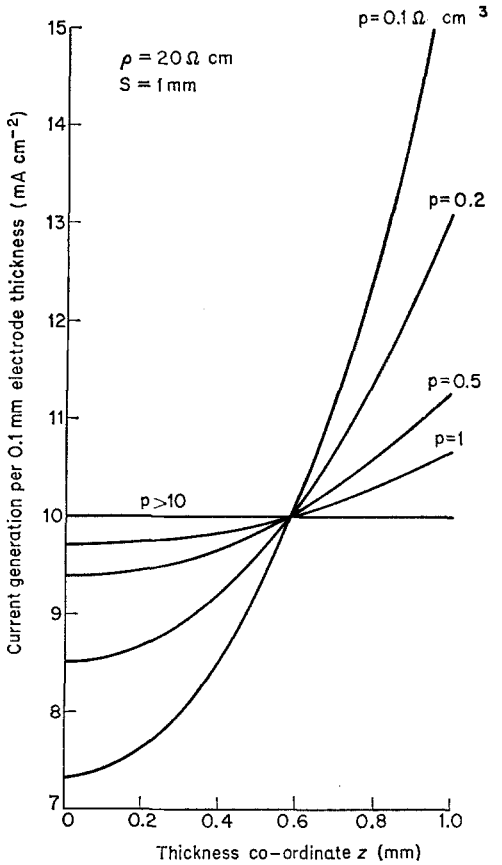

Fig. 5. Examples of the resulting current distribution in flat porous gas electrodes; see Equation (2). Ionic resistivity $\bar{\rho}_i = 20\ \Omega$ cm; thickness $S = 0{\cdot}1$ cm.

can state that for p between 0·5 and 10 Ω cm^3 the distribution remains fairly flat and that the critical values are situated slightly below $p = 0{\cdot}5$ Ω cm^3.

9. Penetration depth

Since the current conversion in the electrodes under consideration is described by monotonous functions without maxima or minima, it may be useful to define a penetration depth Z in the absolute z-scale:

$$\cosh[\sqrt{(\bar{\rho}_i g)}(S-Z)] = \frac{1}{e}\cosh[S\sqrt{(\bar{\rho}_i g)}] \qquad (6)$$

S = electrode thickness
e = basis of natural logarithms
$g = 1/p_i$ = interfacial overvoltage parameter (see p. 108)
$\bar{\rho}$ = steady state ionic resistance.

As evident, this expression loses its significance if cosh $C<$e. Therefore we let the electrode thickness S rise to very high values. Then we are able to replace

$$\cosh [z \gg 1] \approx \frac{1}{2} \exp z, \text{ and we get}$$

$$Z \approx -1/\sqrt{(\bar{\rho}_i g)} \qquad (6a)$$

Table 2. Penetration depth Z of conversion current in working layer of a semi-infinitive porous gas diffusion electrode, as a function of boundary resistance p and specific ionic resistivity $\bar{\rho}_i$.

$p = 1/g$ Ω cm^3	Specific ion resistivity ρ_i (Ω cm) 20	30	40	50	60	80
	Penetration depth Z (mm)					
10	7·02	5·73	4·95	4·45	4·04	3·51
5	5·00	4·08	3·53	3·17	2·89	2·50
2	3·15	2·57	2·22	2·00	1·82	1·58
1	2·25	1·84	1·59	1·42	1·30	1·13
0·5	1·58	1·29	1·12	1·00	0·91	0·79
0·2	1·00	0·82	0·71	0·63	0·58	0·50
0·1	0·70	0·57	0·50	0·44	0·40	0·35
0·05	0·50	0·41	0·35	0·32	0·29	0·25

Table 2 contains calculated penetration depths in the ranges of g and $\bar{\rho}_i$ of interest here. The negative sign is not of importance as it depends only on the chosen co-ordinate direction. Since $\bar{\rho}_i\, g$ increases with rising current density i_s, the penetration depth Z also depends on current density. As an example, see Table 3, which contains experimental values of $\bar{\rho}_i$ and p. It is very difficult and tedious to scrutinize the calculated values for a large number of experimental electrodes. However, we can state, that in the range between 50 and 150 mA cm^{-2}, a thickness of the active electrode layer of more than 0·6 to 0·9 mm has no advantage. Giner and Hunter [15] introduced a similar factor, the 'electrode utilization', which depends also on current density. The authors investigated Teflon-bonded gas electrodes only, whose characteristics differed markedly from those of the hydrophilic nickel electrodes used in this work. Thus it is not possible to compare the present results with those of these authors. In the working layer of manufactured sintered nickel electrodes, penetration depths have been found to be between 0·6 and 0·9 mm. These results refer to electrodes of different design, both oxygen cathodes and hydrogen anodes, containing finely divided silver metal, and Raney nickel as catalysts, respectively. The experimental range of p has to be assumed to be increasing between $0{\cdot}1 < p < 0{\cdot}2$, slowly decreasing with increasing current; see Table 3. Bearing in mind, that under steady load the mean ion resistivity $\bar{\rho}_i$ appears to be somewhat above 20 Ω cm, the measured penetration depths agree fairly well with the results given in Table 2.

Table 3. Calculated penetration depth as a function of current density

Current density i_s (mA cm^{-2})	*Ionic resistivity* $\bar{\rho}_i$ (Ω cm)	$p = 1/g$ (Ω cm^3)	*Penetration depth Z calculated* (mm)
10	20	0·2	1·00
30	21	0·15	0·84
100	22	0·10	0·67
300	25	0·10	0·64

Acknowledgement

This work was carried out at Varta AG, Hannover, Fed. Rep. Germany, and is published by the permission of the Company's Board of Directors, especially Dr Gerhard Lander, Koenigstein. I have to thank a great number of friends and colleagues for helpful comments and discussions, above all Dr Arthur Fleischer, Dr A. A. Pilla, and Prof Dr A. W. Winsel. My sincere thanks are devoted to Dr D. Inman for his valuable help in revising the paper and bringing it into the final version.

References

[1] F. T. Bacon, Brit. Pat. 667 298 (1950).

[2] E. Justi and A. Winsel, 'Kalte Verbrennung'—Fuel Cells (in German), Franz Steiner-Verlag, Wiesbaden, (1962) pp. 88–94.
[3] F. G. Will, *J. Electrochem. Soc.*, **110** (1963) 145.
[4] M. Bonnemay, C. Bernard, G. Bronoel, D. Doniat, E. Levart, G. Peslerbe and A. A. Pilla, 'Etude expérimentale des électrodes poreuses' (in French). 'Les piles à combustible, ouvrage collectif', Paris (1965) pp. 103–125.
[5] R. Buvet, 'Origine des phenomènes de polarisation dans les électrodes poreuses' (in French). 'Les piles à combustible, ouvrage collectif', Paris (1965) pp. 27–46.
[6] A. Winsel, *Advanced Energy Conversion*, **3** (1965) 677; and **5** (1965) 173.
[7] A. Borucka and J. N. Agar, *Electrochimica Acta*, **11** (1966) 603.
[8] L. G. Austin, 'Fuel Cells', NASA S P-120, Washington, D.C. (1967) pp. 303–321.
[9] I. Gurevich and V. S. Bagotskij, *Electrochimica Acta*, **12** (1967) 593.
[10] H. Holthusen, 'Untersuchungen über Knallgaszellen in Eloflux-Anordnung' (in German). Diploma Thesis, Technical University Braunschweig, Fed. Rep. Germany, Dec. 15, 1966 (to be published).
[11] See for instance K. J. Euler and W. Nonnenmacher, *Electrochimica Acta*, **2** (1960) 268.
[12] K. J. Euler and K. N. Mueller, *Electrochimica Acta*, **8** (1963) 949.
[13] K. J. Euler, *Annalen der Physik* (*Leipzig*) **26** (1971), 257.
[14] K. J. Euler, 'Distribution of Current Conversion in Porous Gas Electrodes', American Chemical Society, Preprints of Papers **13** (1969) No. 3, pp. 176–202.
[15] J. Giner and C. Hunter, *J. Electrochem. Soc.*, **116** (1969) 1124.